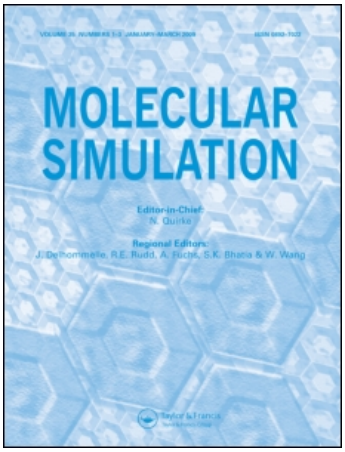

Molecular Simulation
Publication details, including instructions for authors and subscription information:
http://www.informaworld.com/smpp/title~content=t713644482

Electric potential distribution in nanoscale electroosmosis: from molecules to continuum

M. Wang[a]; J. Liu[b]; S. Chen[b]
[a] Nanomaterials in the Environment, Agriculture and Technology (NEAT), University of California, Davis, CA, USA [b] Department of Mechanical Engineering, The Johns Hopkins University, Baltimore, MD, USA

To cite this Article Wang, M. , Liu, J. and Chen, S.(2008) 'Electric potential distribution in nanoscale electroosmosis: from molecules to continuum', Molecular Simulation, 34: 5, 509 — 514
To link to this Article: DOI: 10.1080/08927020701663321
URL: http://dx.doi.org/10.1080/08927020701663321

Molecular Simulation
Vol. 34, No. 5, April 2008, 509–514

Taylor & Francis
Taylor & Francis Group

Electric potential distribution in nanoscale electroosmosis: from molecules to continuum

M. Wang[a,b]*, J. Liu[b] and S. Chen[b,c]

[a]*Nanomaterials in the Environment, Agriculture and Technology (NEAT), University of California, Davis, CA, USA;* [b]*Department of Mechanical Engineering, The Johns Hopkins University, Baltimore, MD, USA;* [c]*College of Engineering and LTCS, Peking University, Beijing, P. R. China*

(*Received 27 May 2007; final version received 3 September 2007*)

Electric potential distribution in nanoscale electroosmosis has been investigated using the nonequilibrium molecular dynamics (NEMD), whose results are compared with the continuum based Poisson–Boltzmann (PB) theory. If the bin size of the MD simulation is no smaller than a molecular diameter and the focusing region is limited to the diffusion layer, the ionic density profiles on the bins of the MD results agree well with the predictions based on the PB theory for low and moderate bulk ionic concentrations. The PB equation breaks down at high bulk ionic concentrations, which is also consistent with the macroscopic description.

Keywords: electric potential distribution; electroosmosis; molecular dynamics; Poisson–Boltzmann theory

PACS: 61.46. + w; 47.60. + i; 61.25. − f

1. Introduction

Electroosmotic transport (EOT) plays a fundamental role in many biochemical and biophysical processes [1,2], such as transports in ion channels in cells [3–5]. Similar applications can also be found in NEMS/MEMS devices [6,7]. A complete understanding of these physical and chemical processes need correct mathematical descriptions and accurate solutions of the electrostatic potential distributions. One of the most widespread models for the electrostatic interactions is the Poisson–Boltzmann equation (PBE) [2]. The linearized PBE (LPBE) and non-linearized PBE (NLPBE) have been used successfully in predictions and modeling of the EOT at microscales [8–10]. However, there are three main defects in the pure continuum approach [11]: (i) the finite sizes of the ions are neglected; (ii) the non-Coulombic interaction between counter- and co-ions and surface is disregarded; (iii) the image forces between ions and the surface are neglected. Although the image charges have been introduced in extensions of Poisson–Boltzmann (PB) theory and more sophistical statistical mechanical treatments of the double layer [12–14], it was generally thought that the PBE broke down in nanoscale EOT.

Much work has been done using the molecular-based simulations with comparisons with the continuum-based PB theory in the last decade [15–23]. Especially, most of the recent papers based on the first principle have reported the PB theory deviates from the MD results in nanoscale electroosmosis [18–23]. Much higher ionic concentration distributions near wall surfaces predicted by MD were reported than those predicted by the PB theory [18,19]. Qiao and Aluru [19] modified the PBE by introducing an electrochemical potential correction extracted from the ion distribution in a smaller channel using MD simulations. The modified PBE predicted the ion distribution in larger channel widths with good accuracies [20,21]. Cui and Cochran [22] found that the PBE agreed quantitatively well with the MD results at moderate ionic concentrations around 20 mM and failed at low ionic concentration and higher zeta potential over 50 mV. Dufreche et al. [23] simulated the electroosmosis in clays, which was simplified as Na^+ ions in water and declared that the PB theory and MD simulation only agreed only when the interlayer spacing was large enough, and that a slipping modification must be considered for the hydrodynamics. Such phenomena can not be explained by the classical electrokinetic transport theories and were ascribed to the water transport properties change near the charged surfaces.

In this paper, we simulate the electroosmosis in nanochannels using the nonequilibrium molecular dynamics (NEMD). The atomic-based results are compared with the continuum based PBE so that the applicability of the continuum assumption is therefore discussed.

2. Numerical details

2.1 Continuum models

Consider an electroosmosis process in a straight channel, as shown in Figure 1. The walls are fixed and homogeneously charged. If the z-directional flow

*Corresponding author. Email: mmwang@ucdavis.edu

ISSN 0892-7022 print/ISSN 1029-0435 online

DOI: 10.1080/08927020701663321
http://www.informaworld.com

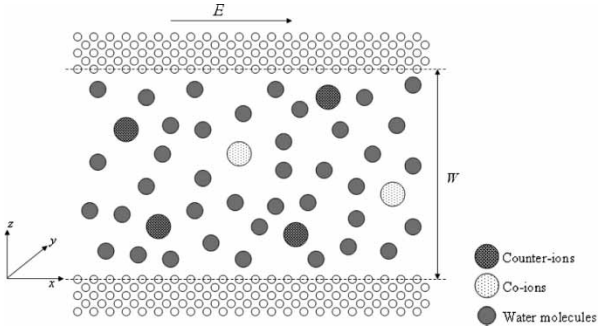

Figure 1. A schematic of the electroosmotic flow in nanochannel. The two channel walls are symmetrical with respect to the channel center line. Each wall is made up of five layers of still solid atoms. The channel width W is defined as the distance between centers in the two innermost wall layers.

is negligible and the transports are periodic in y direction, the steady electrostatic interaction can therefore be described by a 1D Poisson equation [24,25],

$$\frac{\mathrm{d}[\varepsilon_r(z)\mathrm{d}\psi(z)]}{\mathrm{d}z^2} = -\frac{\rho_e}{\varepsilon_0}, \tag{1}$$

where ψ is the electrical potential, ε_r the relative dielectric constant of the solution, ε_0 the permittivity of a vacuum, and ρ_e the net charge density. According to classical EDL theory, the equilibrium Boltzmann distribution function can be used to describe the distributions of small ions in the dilute solution. Therefore, the net charge density distribution can be expressed as the sum of all the ions in the solution

$$\rho_e = \sum_i z_i e n_{i,\infty} \exp\left(-\frac{z_i e}{k_\mathrm{b} T}\psi\right), \tag{2}$$

where the subscript i represents the ith species, n_∞ is the bulk ionic number concentration, z the valence of the ions (including the sign), e the absolute value of one proton charge, k_b the Boltzmann constant and T the absolute temperature. For 1:1 electrolyte solutions, such NaF or NaCl solution in the present work, equations (1) and (2) can be simplified as

$$\frac{\mathrm{d}[\varepsilon_r(z)\mathrm{d}\psi(z)]}{\mathrm{d}z^2} = -\frac{2ze n_\infty}{\varepsilon_0}\sinh\left(\frac{ze\psi}{k_\mathrm{b}T}\right) \tag{3}$$

There are two ways to present the boundary conditions for the Poisson equation (1), Dirichlet and Neumann boundaries. In some atomistic methods for electroosmosis [18,19], the Neumann boundary condition is mostly used because the electric potential gradient is relative to the wall surface charge density. Electric charge conversation can be considered as an additional restrict for certain solution under the Neumann boundary condition, which brings a big additional computational cost as well. Recent investigations show a lattice evolution method can deal with this problem easily [26]. In this contribution we still use the Dirichlet boundary condition to solve the Poisson equation. To compare with the MD simulation results, we obtain the zeta potentials ζ from MD and then use the values as the Dirichlet boundaries to solve the equation (3).

2.2 NEMD method

NEMD method [27] was used to simulate the electroosmosis in a small channel directly. The accuracy of this type of model is limited only by the force fields used to describe interactions between solvent molecules, ions, and the channel walls, and the simulation size and duration, which are determined by computer resources and the computational efficiency of the simulation code. In order to provide a clear picture of how the various conditions affect the applicability of continuum theory, a simplified model was used to capture the essential physics [17,21]. Both solvent and ions are simplified as spherical, nonpolar particles interacting with a shifted Lennard-Jones potential,

$$V^{\mathrm{LJ}}(r_{ij}) = 4\varepsilon_{ij}\left[\left(\frac{\sigma_{ij}}{r_{ij}}\right)^{12} - \left(\frac{\sigma_{ij}}{r_{ij}}\right)^{6} - \left(\frac{\sigma_{ij}}{r_c}\right)^{12} + \left(\frac{\sigma_{ij}}{r_c}\right)^{6}\right], \tag{4}$$

where r_{ij}, ε_{ij} and σ_{ij} are the separation, Lennard-Jones well depth and Lennard-Jones diameter, respectively, for the pair of atoms i and j. With this simplification, the simulations become more tractable while still retaining a model with discrete solvent particles. In deed, replacing such a model for solvent with a more realistic model, such as SPC/E [19,20] will improve the accuracy of the simulations; however the simplified model can still provide qualitative conclusions applicable to real systems, which has been proved in many previous researches for various areas [21]. The L-J interaction is set to zero when molecules are separated by farther than the cut-off length $r_c = 2.5\sigma$. The molecular parameters are chosen to match those in a NaF electrolyte solution in a silicon channel which are listed in Table 1 (http://www.gromacs.org, [28]). The Lorentz–Berthelot combination rules were used for the interaction parameters that are not specified explicitly [28].

Table 1. Parameters for Lennard-Jones interactions between same species particles.

Species	m (g/mol)	σ (Å)	ε (kJ/mol)
O (water)	18.00	3.165	0.6503
Si	28.08	3.386	2.4470
Na^+	22.99	2.350	0.0618
F^-	19.00	3.121	0.6080

Each ion was assigned a charge of $\pm e$ (e is the electronic charge, 1.6×10^{-19} C), while the solvent particles were neutral. The ion–ion electrostatic interactions were calculated using a screened Coulomb interaction,

$$V^{C}(r_{ij}) = \frac{q_i q_j}{4\pi\varepsilon_0\varepsilon_r r_{ij}} \tag{5}$$

where the relative dielectric constant of fluid is approximately set to 78 in our simulations. The electrostatic interactions were computed using the direct summation over the whole domain with no truncation for the Coulomb interactions [29,30].

The equations of motion are integrated using the Verlet scheme [31] with time step $\Delta t = 0.005\tau$, where $\tau \equiv (m\sigma^2/\varepsilon)^{1/2}$ is the characteristic time of the Lennard-Jones potential. A Langevin thermostat [32] with damping rate τ^{-1} is used to maintain a constant temperature of $1.1\varepsilon/k_b$. The thermostat is only applied in the y-direction, since it is periodic and normal to the main flow direction.

NEMD simulations were performed for systems consisting of a slab of electrolyte solution sandwiched by two plane walls as shown in Figure 1. The two walls are symmetrical with respect to the channel center line. Each wall is made up of five layers of atoms oriented in the $<111>$ direction. The channel is L in length and W in width. The wall atoms are fixed to their original positions, all of which have van der Waals interactions with the fluid molecules. Only the outermost wall layers are charged, uniformly among the wall atoms. In cases of this contribution, we use a channel with $L = 3.3$ nm, $W = 4.98$ nm and 1500 molecules flowing in it.

At the beginning of the simulation, the molecules were randomly positioned and assigned Maxwellian distributed velocities at the temperature of $1.1\varepsilon/k_b$. Periodic boundary was performed in the x and y directions. Before the macroscopic characteristics were sampled, the NEMD simulations were run for 5×10^5 time steps to reach steady state flow. After that, the densities and velocities were computed time-averaged, over 3×10^6 times, by using the binning method [31]. The various simulated cases performed in this work are summarized in Table 2.

Table 2. Summary of the simulated cases.

Case #	σ_s (C/m^2)	Counter-ion # (Na^+)	Co-ion # (F^-)
1	0.191	30	0
2	0.191	35	5
3	0.191	40	10
4	0.191	45	15
5	0.191	55	25
6	0.191	80	50
7	0.191	100	70
8	0.191	200	170
9	0.064	10	0
10	0.032	5	0
11	0.019	3	0

3. Results and discussion

3.1 Bin size effect

The electric potential or ion distributions in electroosmosis have been modeled much using atomistic simulations [17–23]. A peak-like and fluctuating ion distribution profile is usually obtained near wall surfaces. The peak values may be two or more times than that predicted by the continuum theory. This was always treated as a proof for breakdown of the PB theory in nanofluidics [18–21]. It was noticed that such a profile always came with a smaller bin size than the fluid molecular diameter. We also got a similar ion distribution profile in a NaF solution by our NEMD when we set the bin size as half of the water molecular diameter, shown as the dotted line in Figure 2. However, when we re-calculated the same results into bigger bin-size systems, the fluctuation became smaller. Once the bin size is no smaller than the fluid molecular diameter, a smooth decaying ion density profile is obtained. Such a profile appears a comparable shape with the PB predictions. It indicates that the base of view must be same when the atomistic simulations are compared with the continuum theory, i.e. the bin size of the MD results of electric distribution should not be smaller than the solvent molecular diameter in comparison with the PB predictions.

3.2 Stern layer effect

A second gap which departs the MD results from the PB predictions is the effect of the Stern layer. As well known,

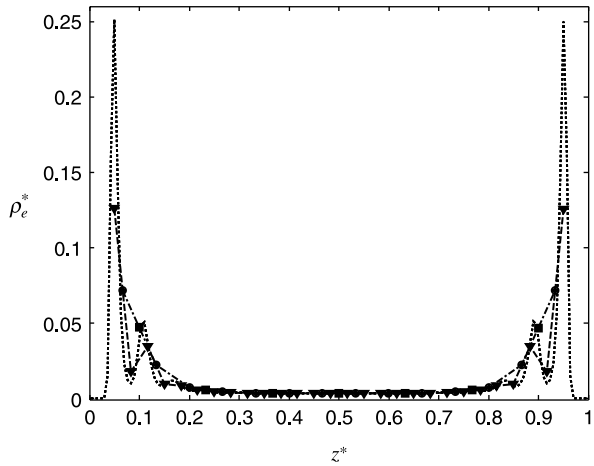

Figure 2. Ion density profiles for different bin sizes(case 1 in Table 2). The ion density is normalized by $|e|/\sigma^3$, i.e. $\rho_e^* = \rho_e/(|e|/\sigma^3)$, and the z-position is normalized by the channel width, e.g. $z^* = z/W$.

the PB equation describes only the ion distribution in diffusion (outer) layer of the electric double layer (EDL) [1,2,24]. In the continuum theory, the compact (inner) layer of EDL is too thin (molecular scale) to be considered and therefore the PB equation almost governs the ion distribution in the whole domain. However, in nanofluidics the inner layer which is also termed as Stern layer is comparable to the channel in size. The PB equation is not able to govern the ion behavior in the Stern layer in theory. Therefore if one compares the MD results with the PB predictions, the Stern layer need to be cut off.

Though the Stern layer is not well defined in theory [33], here we determine its thickness by comparing the co- and counter-ions distribution profiles. The Stern layer is commonly described as the absorbed counter-ions layer close to the charged surface without any co-ions [34,35]. Figure 3 shows the counter-ion and co-ion distribution profiles in the same figure for the NaF solution (case 2 in Table 2). The Stern layer is then determined from the starting point of the counter-ions to that of the co-ions which is almost the first counter-ion layer next to the wall surface. Thus, we compared the MD results ($\delta_{\text{bin}} = \sigma$) with the PB predictions in the whole channel or in the diffusion layers only. Figure 4 shows that the MD results deviates far from the PB prediction in the whole channel, however agree pretty well with those in the diffusion layers only for this case. This indicates that when the Stern layer is not negligible compared with the channel width, the PB theory can not predict the ion distribution correctly across the whole channel but it is still available to describe the electric potential distribution in the diffusion layers. Once the channel is so narrow that the Stern layers near both wall surfaces have interactions with each other, such as $W < 5\sigma$, the PB theory will totally break down across the channel. Such a deduction is consistent with the previous MD simulations [19].

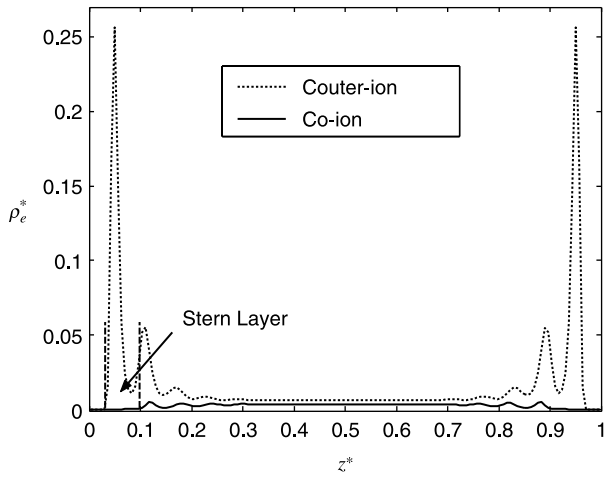

Figure 3. Stern layer determination from MD results (case 2 in Table 2).

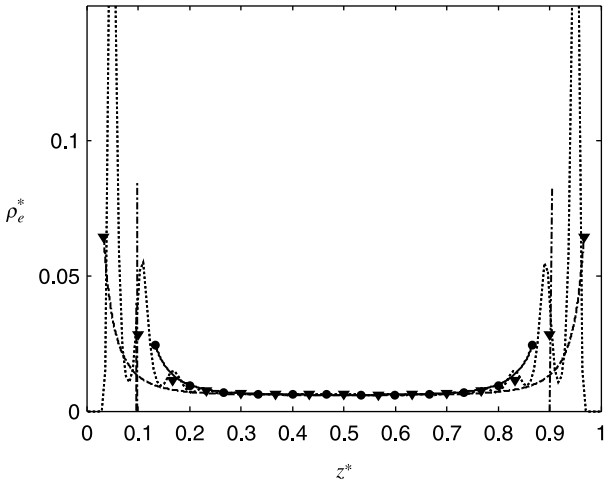

Figure 4. Comparisons between MD and Poisson–Boltzmann theory: the dotted line is the MD results in finest bin size, the circles and triangles are sampled in one molecular diameter bin size. The triangles are sampled in the whole channel width W, and the circles are sampled only in the diffusion layer. The dot-dash lines are the interfaces between stern layer and diffusion layer. The dashed line and solid line are calculated based on PB equation for different channel widths and different zeta potentials. (case 2 in Table 2).

3.3 Concentration effect

In theory, the PBE is based on the Boltzmann distribution of ions for dilute solutions. The assumption of dilute solution is almost satisfied in most macroscopic cases; however it becomes somewhat critical for nanoscale electroosmosis. In this contribution, we change the numbers of ions in the solution so as to see how far the PBE holds on by comparing the MD results with the PB predictions. The bulk ionic concentration is determined by the averaged ion concentration in equilibrium far from the wall surfaces (i.e. near the middle across the channel) of the MD results. Thus, the cases listed in Table 2 have a wide bulk ionic concentration range from 0.1 to 5.25 M. Figure 5 shows the PBE holds on for low and moderate ionic concentrations. When the bulk ionic concentration is lower than 0.88 M (case 5), the PB predictions agree well with the MD results, see Figure 5(a). As the ionic concentration increasing, the deviations become larger and larger, which indicates the Boltzmann distribution breaks down and the PB theory can not describe such electrokinetic transport behavior any more.

4. Conclusions

Electric potential distribution in nanoscale electroosmosis have been numerically investigated using both the atomistic method NEMD and the continuum theory PBE. The applicability of the continuum-based PB theory

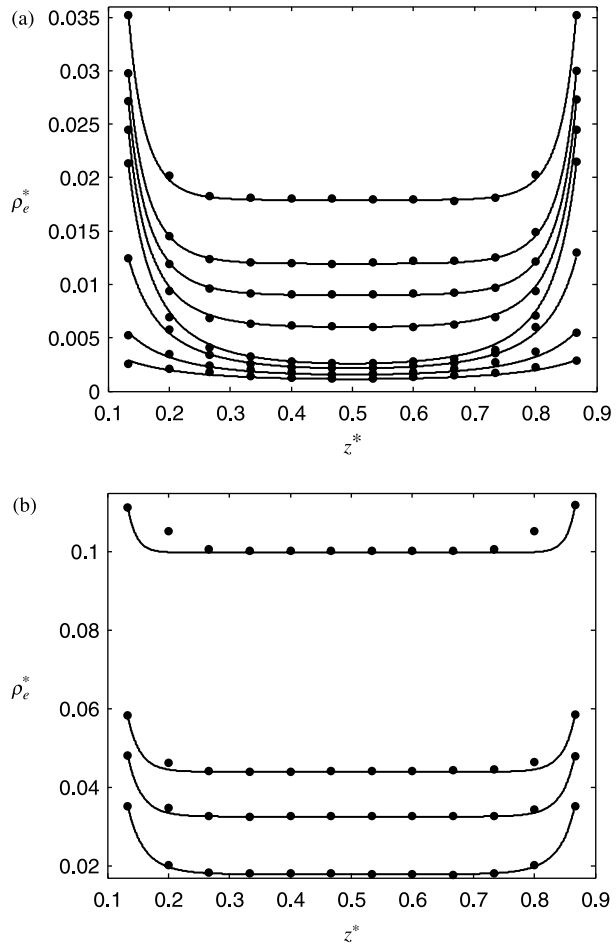

Figure 5. Ionic density profiles from MD simulations and PB predictions for different ionic concentration cases. (a) cases at moderate and low ionic concentrations. The cases from bottom to top are: cases # 11, 10, 9, 1, 2, 3, 4, 5. The bulk ionic concentration of case 5 is 0.88 M; (b) cases at high ionic concentrations. The cases from bottom to top are: cases # 5, 6, 7, 8.

in nanoscale is therefore discussed by comparing the results from the two different methods. The results show that: if the bin size of the MD simulation is no smaller than a molecular diameter of solvent and the focusing region is limited to the diffusion layer, the ion distribution profiles calculated by MD simulations agree well with PB predictions at low and moderate bulk ionic concentrations. The PB theory totally breaks down for high bulk ionic concentrations, which is also consistent with the macroscopic description.

References

[1] K.A. Sharp and B. Honig, *Electrostatic interactions in macromolecules—theory and applications*, Annu. Rev. Biophys. Biophys. Chem. 19 (1990), pp. 301–332.

[2] B. Honig and A. Nicholls, *Classical electrostatics in biology and chemistry*, Science 268(5214) (1995), pp. 1144–1149.

[3] S. Kuyucak and T. Bastug, *Physics of ion channels*, J. Biol. Phys. 29 (2003), pp. 429–446.

[4] B. Roux, *Ion conduction and selectivity in K+ channels*, Annu. Rev. Biophys. Biomol. Struct. 34 (2005), pp. 153–171.

[5] D.E. Draper, D. Grilley, and A.M. Soto, *Ions and RNA folding*, Annu. Rev. Biophys. Biomol. Struct. 34 (2005), pp. 221–243.

[6] P.K. Wong, T.H. Wang, J.H. Deval, and C.M. Ho, *Electrokinetics in micro devices for biotechnology applications*, IEEE–ASME Trans. Mechatron. 9(2) (2004), pp. 366–376.

[7] M. Wang, J.K. Wang, S.Y. Chen, and N. Pan, *Electrokinetic pumping effects of charged porous media in microchannels using the lattice Poisson–Boltzmann method*, J. Colloid Interface Sci. 304(1) (2006), pp. 246–253.

[8] D.Q. Li, *Electro-viscous effects on pressure-driven liquid flow in microchannels*, Colloid Surf. A 195 (2001), pp. 35–57.

[9] R.J. Flatt and P. Bowen, *Electrostatic repulsion between particles in cement suspensions: domain of validity of linearized Poisson–Boltzmann equation for nonideal electrolytes*, Cem. Concr. Res. 33 (2003), pp. 781–791.

[10] J.K. Wang, M. Wang, and Z.X. Li, *Lattice Poisson–Boltzmann simulations of electro-osmotic flows in microchannels*, J. Colloid Interface Sci. 296(2) (2006), pp. 729–736.

[11] J. Yang, *Surface effects of microchannel wall on microfluidics*, Ph.D. thesis, University of Alberta, 2004.

[12] P. Attard, D.J. Mitchell, and B.W. Ninham, *Beyond Poisson–Boltzmann—Images and correlations in the electric double layer. 1. Counterions only*, J. Chem. Phys. 88(8) (1988), pp. 4987–4996.

[13] ———, *Beyond Poisson–Boltzmann—Images and correlations in the electric double layer. 2. Symmetric electrolyte*, J. Chem. Phys. 89(7) (1988), pp. 4358–4367.

[14] L.M. Varela, M. Garcia, and V. Mosquera, *Exact mean-field theory of ionic solutions: non-Debye screening*, Phys. Rep. Rev. Sect. Phys. Lett. 382(1–2) (2003), pp. 1–111.

[15] W.Y. Lo, K.Y. Chan, and K.L. Mok, *Molecular dynamics simulation of ions in charged capillaries*, J. Phys. Condens. Matter. 6 (1994), pp. A145–A149.

[16] W.Y. Lo, K.Y. Chan, M. Lee, and K.L. Mok, *Molecular simulation of electrolytes in nanopores*, J. Electroanal. Chem. 450 (1998), pp. 265–272.

[17] A.P. Thompson, *Nonequilibrium molecular dynamics simulation of electro-osmotic flow in a charged nanopore*, J. Chem. Phys. 119(14) (2003), pp. 7503–7511.

[18] J.B. Freund, *Electro-osmosis in a nanometer-scale channel studied by atomistic simulation*, J. Chem. Phys. 116(5) (2002), pp. 2194–2200.

[19] R. Qiao and N.R. Aluru, *Ion concentrations and velocity profiles in nanochannel electroosmotic flows*, J. Chem. Phys. 118(10) (2003), pp. 4692–4701.

[20] ———, *Scaling of electrokinetic transport in nanometer channels*, Langmuir 21(19) (2005), pp. 8972–8977.

[21] W. Zhu, S.J. Singer, Z. Zheng, and A.T. Conlisk, *Electro-osmotic flow of a model electrolyte*, Phys. Rev. E 71 (2005), 041501.

[22] S.T. Cui and H.D. Cochran, *Electroosmotic flow in nanoscale parallel-plate channels: molecular simulation study and comparison with classical Poisson–Boltzmann theory*, Mol. Simul. 30(5) (2004), pp. 259–266.

[23] J.F. Dufreche, V. Marry, N. Malikova, and P. Turq, *Molecular hydrodynamics for electro-osmosis in clays: from Kubo to Smoluchowski*, J. Mol. Liq. 118 (2005), pp. 145–153.

[24] J.H. Masliyah, *Electrokinetic Transport Phenomena*, Alberta Oil Sands Technology and Research Authority, Alberta, Canada, 1994.

[25] S. Levine, J.R. Marriott, and K. Robinson, *Theory of electrokinetic flow in a narrow parallel-plate channel*, J. Chem. Soc. Faraday Trans. 71 (1975), pp. 1–11.

[26] J.K. Wang, M. Wang, and Z.X. Li, *Lattice evolution solution for the non-linear Poisson–Boltzmann equation in confined domains*, Commun. Nonlinear Sci. Numer. Simulat. doi: 10.1016/j.cnsns.2006.06.002 (2007).

[27] P.A. Thompson and M.O. Robbins, *Shear-flow near solids: eptaxial order and flow boundary conditions*, Phys. Rev. A 41(12) (1990), pp. 6830–6837.

[28] M. Patra and M. Karttunen, *Systematic comparison of force fields for microscopic simulations of NaCl in aqueous solutions: diffusion, free energy of hydration, and structural properties*, J. Comput. Chem. 25 (2004), pp. 678–689.

[29] H. Dufner, S.M. Kast, J. Brickmann, and M. Schlenkrich, *Ewald summation versus direct summation of shifted-force potentials for the calculation of electrostatic interactions in solids: a quantitative study*, J. Comput. Chem. 18(5) (1997), pp. 660–676.
[30] M. Wang, J. Liu, and S. Chen, *Similarity of electroosmotic flows in nanochannels*, Mol. Simul. 33(3) (2007), pp. 239–244.
[31] M. Allen and D. Tildesley, *Computer Simulations of Liquids*, Oxford University Press, New York, 1987.
[32] G.S. Grest and K. Kremer, *Molecular dynamics simulation of polymers in the presence of a heat bath*, Phys. Rev. A 33 (1986), pp. 3628–3631.
[33] M. Bazart, *Department of Mechanical Engineering*, MIT, Personal communications 2005.
[34] C.S. Mangelsdorf and L.R. White, *Effects of Stern-layer conductance on electrokinetic transport—properties of colloids particles*, J. Chem. Soc. Faraday Trans. 86(16) (1990), pp. 2859–2870.
[35] ———, *The dynamic double layer-Part 2-effects of Stern-layer conduction on the high-frequency electrokinetic transport properties*, J. Chem. Soc. Faraday Trans. 94(17) (1998), pp. 2583–2593.
[36] K.P. Travis and K.E. Gubbins, *Poiseuille flow of Lennard-Jones fluids in narrow slit pores*, J. Chem. Phys. 112(4) (2000), pp. 1984–1994.